THEORETICAL STUDY FOR THE FLOW IN THE GAP BETWEEN CONCENTRIC SPHERES, ONE OF WHICH ROTATES

KOICHI NAKABAYASHI
Department of Mechanical Engineering

(Received August 28, 1984)

The flow between concentric spheres, one of which rotates, is considered theoretically on the assumption that the space between the two spheres is relatively small in comparison to radial dimensions, where Navier-Stokes equations can be reduced to a relatively simple form through order-of-magnitude arguments. These simplified equations are integrated by the perturbation method.

In addition to the velocity component in the direction of rotation, secondary velocity components are also present for large Reynolds number. These velocity components, shearing stress, pressure distribution and viscous frictional moment (torque) are obtained. Upon comparison, the theoretical results are found to agree well with the experimental data, being within $R_e\beta^2 < 40$.

1. INTRODUCTION

Recently, interest has been focused upon the flow in the narrow space between two bodies, which rotate about a common axis. These narrow spaces found in turbomachinery are not only linear, as with rotating disks or cones, but also curvilinear, as is the case between two spheres. There are many problems to be solved as to the flow in such curvilinear space. As one consideration on the rotating fluids in the space between two spherical surfaces, we herewith consider the flow of an incompressible viscous fluid contained between two concentric spheres, one of which rotates about a common axis.

The flow between concentric rotating spheres is very interesting for engineering and geophysics, in particular. Fluid motion in a rotating spherical annulus has been chiefly investigated as to hydrodynamic stability or atmospheric and oceanic circulation from the viewpoint of geophysics, considering, for example, the case in which a large clearance between spheres is equal to the radius of the inner sphere. Pearson (1967) or Munson and Joseph (1971) proposed computational methods, by which full Navier-Stokes eqs. can be integrated numerically in the above-mentioned problems, but their methods are complicated and computers have to be used. Most of these studies, however, involve an outer sphere with a radius twice that of the inner one, and it is difficult to theoretically formulate frictional resistance, velocity etc. for annular space narrow enough to serve as the focus for mechanical engineering considerations. Moreover, the space ratio, Reynolds number and the like which affect the flow are not fully explained. Although Sawatzki and Zierep (1970) have investigated both experimentally and theoretically the flow in narrow spherical annuli between concentric spheres, with the inner one rotating, their theoretical consideration seems to be inapplicable to large Reynolds number. In their analysis the boundary layer's eqs. obtained by Howarth (1951) was used, where the pressure gradient in the θ-direction is neglected. They obtained the result that the velocity component in the ϕ-direction is not influenced by the secondary flow. But the experimental results of the coefficient of frictional moment are influenced by the secondary flow and tend to increase for the larger Reynolds number above a critical value for each clearance ratio ; and the pressure distribution in the θ-direction is not obtained, either

In this report, in order to improve on the above-mentioned points, Navier-Stokes eqs. were reduced by order-of-magnitude estimates, assuming that the clearance between spheres is small enough in relation to the radius of the inner sphere. The solution was obtained by a perturbation technique. Velocity components, shearing stress, frictional moment and pressure distribution were obtained.

NOTATION

C_M	= coefficient of viscous frictional moment, $M/\ (\rho R_1^5\omega^2)$
f_{jl}	= function of η
g_{jl}	= function of η
M	= viscous frictional moment
p	= pressure
P_j	= jth-order Legendre polynomial
$r,\ \theta,\ \phi$	= spherical polar coordinates, Fig. 1
$R_1,\ R_2$	= radii of inner and outer spheres
R_e	= Reynolds number based on the radius of inner sphere, $R_1^2\omega/\nu$
R_s	= Reynolds number based on clearance s between inner and outer sphere, $R_1\omega s/\nu=R_e\beta$
s	= clearance between inner and outer sphere, R_2-R_1
$u,\ v,\ w$	= velocity components in the ϕ, θ and r-directions
y	= distance from the inner sphere, $r-R_1$
β	= clearance ratio, s/R_1
η	= dimensionless y-coordinate, y/s
μ	= dynamic viscosity
ν	= kinematic viscosity
ρ	= density
$\tau_{r\phi}$	= wall shear stress of inner sphere in the ϕ-direction
ψ	= stream function
ω	= angular velocity of outer sphere or inner one
Ω	= angular velocity function

Subscript

* nondimensional variables

2. ANALYSIS

Using the nomenclature given in Fig. 1 and assuming axial symmetry, the governing equations expressed in the spherical coordinate system are reduced from full Navier-Stokes equations and continuity equation as follows.

$$\underset{o(\delta^2)}{w\frac{\partial w}{\partial r}}+\underset{o(\delta)}{\frac{v}{r}\frac{\partial w}{\partial \theta}}-\underset{o(1)}{\frac{v^2+u^2}{r}}=-\frac{1}{\rho}\frac{\partial p}{\partial r}+\nu\{\underset{o(\delta^{-1})}{\frac{1}{r^2}\frac{\partial p}{\partial r}(r^2\frac{\partial w}{\partial r})}$$

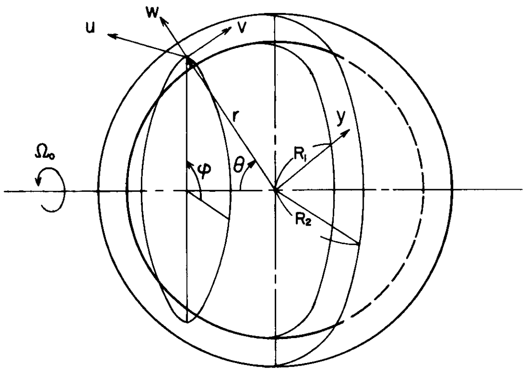

Fig. 1 Spherical annulus.

$$+\underset{o(\delta)}{\frac{1}{r^2\sin\theta}\frac{\partial}{\partial\theta}(\sin\theta\frac{\partial w}{\partial\theta})}-\underset{o(\delta)}{\frac{2w}{r^2}}-\underset{o(1)}{\frac{2}{r^2}\frac{\partial v}{\partial\theta}}-\underset{o(1)}{\frac{2v\cot\theta}{r^2}}\},\quad (1\ a)$$

$$\underset{o(1)}{w\frac{\partial v}{\partial r}}+\underset{o(1)}{\frac{v}{r}\frac{\partial v}{\partial\theta}}-\underset{o(1)}{\frac{u^2\cot\theta}{r}}+\underset{o(\delta)}{\frac{wv}{r}}=-\frac{1}{\rho r}\frac{\partial p}{\partial\theta}$$

$$+\nu\{\underset{o(\delta^2)}{\frac{1}{r^2}\frac{\partial}{\partial r}(r^2\frac{\partial v}{\partial r})}+\underset{o(1)}{\frac{1}{r^2\sin\theta}\frac{\partial}{\partial\theta}(\sin\theta\frac{\partial v}{\partial\theta})}$$

$$+\underset{o(\delta)}{\frac{2}{r^2}\frac{\partial w}{\partial\theta}}-\underset{o(1)}{\frac{v}{r^2\sin^2\theta}}\},\qquad (1\ b)$$

$$\underset{o(1)}{w\frac{\partial u}{\partial r}}+\underset{o(1)}{\frac{v}{r}\frac{\partial u}{\partial\theta}}+\underset{o(\delta)}{\frac{uw}{r}}+\underset{o(1)}{\frac{uv\cot\theta}{r}}=\nu\{\underset{o(\delta^2)}{\frac{1}{r^2}\frac{\partial}{\partial r}(r^2\frac{\partial u}{\partial r})}$$

$$+\underset{o(1)}{\frac{1}{r^2\sin\theta}\frac{\partial}{\partial\theta}(\sin\theta\frac{\partial u}{\partial\theta})}-\underset{o(1)}{\frac{u}{r^2\sin^2\theta}}\},\qquad (1\ c)$$

$$\underset{o(1)}{\frac{1}{r}\frac{\partial}{\partial r}(r^2w)}+\underset{o(1)}{\frac{1}{\sin\theta}\frac{\partial}{\partial\theta}(v\sin\theta)}=0,\qquad (2)$$

where the clearance s between two spheres is very small in comparison with R_1 or R_2, Eqs. (1) and (2) can be simplified by an order-of-magnitude estimate. Substituting $r=R_1+y$, Eq. (2) becomes

$$\frac{2w}{R_1}+(1+\frac{y}{R_1})\frac{\partial w}{\partial y}+\frac{1}{R_1\sin\theta}\frac{\partial}{\partial\theta}(v\sin\theta)=0.\qquad (3)$$

An order-of-magnitude estimate of the size of individual terms in Eq. (3) is made for the relative sizes of u, v, w and their derivatives. Thus, u, v, R_1 and θ are assumed to be of the order (1), y of the order (δ), and δ is taken as a very minute quantity compared to unity, which is equivalent to the clearance ratio β. From Eq. (3), w is also assigned the order (δ). Hence, Eq. (3) becomes

$$\frac{\partial w}{\partial y}+\frac{1}{R_1 sin\ \theta}\frac{\partial}{\partial\theta}(vsin\ \theta)=0. \tag{4}$$

Substituting $r=R_1+y$ into Eq. (1), comparing the order-of-magnitude of individual terms in Eq. (1) and leaving the terms of the maximum order of δ, the equations of motion are reduced to

$$\underset{o(1)}{\frac{u^2+v^2}{R_1}}=\frac{1}{\rho}\frac{\partial p}{\partial y}-\underset{\nu\cdot o(\delta^{-1})}{\nu\frac{\partial^2 w}{\partial y^2}}, \tag{5 a}$$

$$\underset{o(1)}{w\frac{\partial v}{\partial y}}+\underset{o(1)}{\frac{v}{R_1}\frac{\partial v}{\partial\theta}}-\underset{o(1)}{\frac{u^2 cot\ \theta}{R_1}}=-\frac{1}{\rho R_1}\frac{\partial p}{\partial\theta}+\underset{\nu\cdot o(\delta^{-2})}{\nu\frac{\partial^2 v}{\partial y^2}}, \tag{5 b}$$

$$\underset{o(1)}{w\frac{\partial u}{\partial y}}+\underset{o(1)}{\frac{v}{R}\frac{\partial u}{\partial\theta}}+\underset{o(1)}{\frac{uvcot\ \theta}{R_1}}=\underset{\nu\cdot o(\delta^{-2})}{\nu\frac{\partial^2 u}{\partial y^2}}. \tag{5 C}$$

Assuming $\nu\sim o(\delta^2)$ and $\rho\sim o(1)$ in Eq. (5), the relation of $p\sim o(\delta)$ can be obtained from Eq. (5 a). Then the pressure term in Eq. (5 b) can be neglected and the Eqs. (5 b) and (5 c) agree with the equations of boundary layer obtained by Howarth (1951). Now, assuming $\nu\sim o(\delta)$ instead of $\nu\sim o(\delta^2)$, we can get the linear distribution of u, $v=0$ and $w=0$, i. e. the velocity distribution of creeping motion. The purpose of the present paper is to show how an analytic perturbation solution is given to the increase of Reynolds number and clearance ratio, so that ν is properly considered to be a parameter whose order-of-magnitude is variable from $o(\delta)$ to $o(\delta^2)$. Hence the pressure terms of Eqs. (5 a) and (5 b) remain, but the term $\nu\partial^2 w/\partial y^2$ in Eq. (5 a) is omitted in order to simplify the equation.

The equations to be solved are given by

$$\frac{u^2+v^2}{R_1}=\frac{1}{\rho}\frac{\partial p}{\partial y}, \tag{6 a}$$

$$w\frac{\partial v}{\partial y}+\frac{v}{R_1}\frac{\partial v}{\partial\theta}-\frac{u^2 cot\ \theta}{R_1}=-\frac{1}{\rho R_1}\frac{\partial p}{\partial\theta}+\nu\frac{\partial^2 v}{\partial y^2}, \tag{6 b}$$

$$w\frac{\partial u}{\partial y}+\frac{v}{R_1}\frac{\partial u}{\partial\theta}+\frac{uvcot\ \theta}{R_1}=\nu\frac{\partial^2 u}{\partial y^2}. \tag{6 c}$$

Velocity components u, v and w can be related to Ψ and Ω by

$$v=-\frac{1}{sin\ \theta}\frac{\partial\Psi}{\partial y}, \tag{7 a}$$

$$w=\frac{1}{R_1 sin\ \theta}\frac{\partial\Psi}{\partial\theta}, \tag{7 b}$$

$$u=\frac{\Omega}{R_1 sin\ \theta}, \tag{7 c}$$

where v and w satisfy Eq. (4). The governing equations are made dimensionless by the use of

$$\frac{y}{s}=\eta,\ \frac{u}{R_1\omega}=u^*,\ \frac{v}{R_1\omega}=v^*,\ \frac{w}{R_1\omega}=w^*,$$
$$\frac{p}{\rho R_1{}^2\omega^2}=p^*,\ \frac{\Psi}{R_1{}^2\omega}=\Psi^*,\ \frac{\Omega}{R_1{}^2\omega}=\Omega^*, \tag{8}$$

to give the following equations :

$$\beta(u^{*2}+v^{*2})=\frac{\partial p^*}{\partial\eta}-\frac{1}{R_s}\frac{\partial^2 w^*}{\partial\eta^2}, \tag{9 a}$$

$$w^*\frac{\partial v^*}{\partial\eta}+\beta v^*\frac{\partial v^*}{\partial\theta}-\beta u^{*2}cot\ \theta=-\beta\frac{\partial p^*}{\partial\theta}+\frac{1}{R_s}\frac{\partial^2 v^*}{\partial\eta^2}, \tag{9 b}$$

$$w^*\frac{\partial u^*}{\partial\eta}+\beta v^*\frac{\partial u^*}{\partial\theta}+\beta u^* v^* cot\ \theta=\frac{1}{R_s}\frac{\partial^2 u^*}{\partial\eta^2}, \tag{9 c}$$

$$v^*=\frac{-1}{\beta sin\theta}\frac{\partial\Psi^*}{\partial\eta}, \tag{10 a}$$

$$w^*=\frac{1}{sin\ \theta}\frac{\partial\Psi^*}{\partial\theta}, \tag{10 b}$$

$$u^*=\frac{\Omega^*}{sin\ \theta}. \tag{10 c}$$

Eliminating p^* from Eqs. (9 a) and (9 b) and using the relationship given by Eq. (10), the governing equations become

$$2\beta^3(\Omega^*\frac{\partial\Omega^*}{\partial\theta}-\Omega^{*2}cot\ \theta)-2\beta^2\Omega^*\frac{\partial\Omega^*}{\partial\eta}cot\ \theta$$
$$+2\beta\{\frac{\partial\Psi^*}{\partial\eta}\frac{\partial^2\Psi^*}{\partial\eta\partial\theta}-(\frac{\partial\Psi^*}{\partial\eta})^2 cot\ \theta\}$$
$$-2\frac{\partial\Psi^*}{\partial\eta}\frac{\partial^2\Psi^*}{\partial\eta^2}cot\theta-\frac{\partial\Psi^*}{\partial\theta}\frac{\partial^3\Psi^*}{\partial\eta^3}+\frac{\partial\Psi^*}{\partial\theta}\frac{\partial^3\Psi^*}{\partial\eta^2\partial\theta}$$
$$=-\frac{1}{R_s}\frac{\partial^4\Psi^*}{\partial\eta^4}sin\ \theta, \tag{11 a}$$

$$\frac{\partial\Psi^*}{\partial\theta}\frac{\partial\Omega^*}{\partial\eta}-\frac{\partial\Psi^*}{\partial\eta}\frac{\partial\Omega^*}{\partial\theta}=\frac{sin\ \theta}{R_s}\frac{\partial^2\Omega^*}{\partial\eta^2}. \tag{11 b}$$

The solution for these equations is obtained by a perturbation technique. The perturbation solution of equation (11) can be written in the form of Munson and Joseph (1971) ;

$$\Psi^*(\eta,\theta)=sin^2\theta\sum_{\substack{l=1\\ odd}}^{\infty}R_s^l\{\sum_{\substack{j=1\\ odd}}^{l}P_j(cos\theta)g_{jl}(\eta)\}, \tag{12}$$

$$\Omega^*(\eta,\theta)=sin^2\theta\sum_{\substack{l=0\\ even}}^{\infty}R_s^l\{\sum_{\substack{j=0\\ even}}^{l}P_j(cos\theta)f_{jl}(\eta)\}, \tag{13}$$

where $P_j(cos\theta)$ is the jth-order Legendre polynomial, and both $g_{jl}(\eta)$ and $f_{jl}(\eta)$ are functions of η. Considering the convergency of Eqs. (12) and (13), we have to take account of not only R_s, but also β

in the functions, $g_{jl}(\eta)$ and $f_{jl}(\eta)$, as can be seen in Eq. (22). Substituting equations (12) and (13) into Eq. (11) and equating equal powers of R_s, the system of equations is multiplied by an appropriate Legendre polynomial, $P_m(\cos\theta)$, and integrated ($0 \leqq \theta \leqq \pi$). Using the orthogonal properties, the pertubation equations can be written as follows.

At R_s^{-1},

$$\frac{d^2 f_{00}}{d\eta^2} = 0. \tag{14}$$

At R_s^0,

$$\frac{d^4 g^{11}}{d\eta^4} = 2\beta^2 f_{00}\frac{df_{00}}{d\eta} 2\beta^3 f_{00}{}^2. \tag{15}$$

At R_s^1,

$$\frac{d^2 f_{02}}{d\eta^2} = -\frac{2}{3}f_{00}\frac{dg_{11}}{d\eta}, \tag{16}$$

$$\frac{d^2 f_{22}}{d\eta^2} = 2g_{11}\frac{df_{00}}{d\eta} - \frac{4}{3}f_{00}\frac{dg_{11}}{d\eta}. \tag{17}$$

At R_s^2,

$$\frac{d^4 g_{13}}{d\eta^4} = \frac{2}{5}\frac{dg_{11}}{d\eta}\frac{d^2 g_{11}}{d\eta^2} + \frac{4}{5}g_{11}\frac{d^3 g_{11}}{d\eta^3} - \frac{2}{5}\left(\frac{dg_{11}}{d\eta}\right)^2 + \beta^2\left\{f_{00}\left(2\frac{df_{02}}{d\eta} + \frac{4}{5}\frac{df_{22}}{d\eta}\right) + \frac{df_{00}}{d\eta}\left(2f_{02} + \frac{4}{5}f_{22}\right)\right\} + \beta^3 f_{00}\left(-4f_{02} + \frac{4}{5}f_{22}\right). \tag{18}$$

$$\frac{d^4 g_{33}}{d\eta^4} = -\frac{2}{5}\frac{dg_{11}}{d\eta}\frac{d^2 g_{11}}{d\eta^2} + \frac{6}{5}g_{11}\frac{d^3 g_{11}}{d\eta^3} - \frac{8}{5}\beta\left(\frac{dg_{11}}{d\eta}\right)^2 + \frac{6}{5}\beta^2\left\{f_{00}\frac{df_{22}}{d\eta} + f_{22}\frac{df_{00}}{d\eta}\right\} - \frac{14}{5}\beta^3 f_{00} f_{22}. \tag{19}$$

3. SOLUTIONS

3.1 WITH THE OUTER SPHERE ROTATING

The boundary conditions are given by

$$u^* = v^* = w^* = 0 \quad \text{at } \eta = 0, \qquad u^* = (1+\beta)\sin\theta,\ v^* = w^* = 0 \quad \text{at } \eta = 1, \tag{20}$$

The boundary conditions corresponding to both g_{jl} and f_{jl} can be written at $\eta = 0$:

$g_{jl} = 0$, $dg_{jl}/d\eta = 0$, where both j and l are odd ;
$f_{jl} = 0$, where both j and l are even ; (21 a)

And at $\eta = 1$,

$g_{jl} = 0$, $dg_{jl}/d\eta = 0$, where both j and l are odd ;
$f_{00} = (1+\beta)$, $f_{jl} = 0$, (21 b)

where both j and l are even except for 0.

Integrating equations (14)−(19) with the boundary conditions (21), solutions for component functions f_{jl} and g_{jl} are obtained as follows :

$$f_{00} = (1+\beta)\eta, \tag{22 a}$$

$$g_{11} = \beta^2(1+\beta)^2\left\{-\frac{\beta}{180}\eta^6 + \frac{1}{60}\eta^5 + \frac{1}{45}\left(\beta - \frac{9}{4}\right)\eta^3 - \frac{1}{60}(\beta - 2)\right\}\eta^2, \tag{22 b}$$

$$f_{02} = \beta^2(1+\beta)^3 10^{-3}\{0.39683\beta\eta^8 - 1.32287\eta^7 + (5 - 2.2222\beta)\eta^5 + (1.8519\beta - 3.7037)\eta^4 + (0.026455 - 0.026455\beta)\eta\}, \tag{22 c}$$

$$f_{22} = \beta^2(1+\beta)^3 10^{-3}\{0.59524\beta\eta^8 - 1.8519\eta^7 + (5 - 2.2222\beta)\eta^5 + (0.92593\beta - 1.8519)\eta^4 + (0.70106\beta - 1.2963)\eta\}, \tag{22 d}$$

$$g_{13} = \beta^4(1+\beta)^4 10^{-5}\{-0.09152\beta\eta^{12} - 0.10823\eta^{11} + 0.615079\beta\eta^{10} + (0.33069 - 0.61728\beta)\eta^9 - (0.39683 + 0.8664\beta)\eta^8 + (3.5714 - 2.2222\beta)\eta^7 - (5.5555 - 4.4358\beta)\eta^6 - (0.15875 + 0.10503\beta)\eta^5 + (5.88151 - 0.80074\beta)\eta^3 - (3.56427 + 0.3469\beta)\eta^2\}, \tag{22 e}$$

$$g_{33} = \beta^4(1+\beta)^4 10^{-5}\{-0.07994\beta\eta^{12} - 0.11224\eta^{11} + 0.6746\beta\eta^{10} - 1.12189\beta\eta^9 + (1.05819 - 2.672\beta)\eta^8 - 3.8095\beta\eta^7 - 0.96706\beta\eta^6 + (4.0740 + 0.66139\beta)\eta^5 + (6.883 + 40.219\beta)\eta^3 - (3.7549 + 32.905\beta)\eta^2\}. \tag{22 f}$$

Substituting above equations into Eqs. (12) and (13), Ψ^* and Ω^* can be obtained. Then, using Eq. (10) and $R_s = R_e\beta$, we may write v^*, w^* and u^* by

$$v^* = -R_e\sin\theta\cos\theta\frac{dg_{11}}{d\eta} - \beta^2 R_e^3\left\{\sin\theta\cos\theta\frac{dg_{13}}{d\eta} + \frac{1}{8}\sin\theta(5\cos3\theta + 3\cos\theta)\frac{dg_{33}}{d\eta}\right\} + \cdots, \tag{23 a}$$

$$w^* = \beta R_e g_{11}(3\cos^2\theta - 1) + \beta^3 R_e^3\left\{g_{13}(3\cos^2\theta - 1) + \frac{1}{4}g_{33}\cos\theta(5\cos3\theta + 3\cos\theta) - \frac{3}{8}g_{33}\sin\theta(5\sin3\theta + \sin\theta)\right\} + \cdots, \tag{23 b}$$

$$u^* = f_{00}\sin\theta + \beta^2 R_e^2\left\{f_{02}\sin\theta + \frac{f_{22}}{4}\sin\theta(3\cos2\theta + 1)\right\} + \cdots, \tag{23 c}$$

where g_{11}, g_{13}, f_{00}, f_{02}, etc. are given by Eq. (22). Substituting $R_e = 0$ into Eq. (23), v^*, w^* and u^* become

$$v^* = w^* = 0,\quad u^* = (1+\beta)\eta\ \sin\theta. \tag{24}$$

This shows a velocity distribution similar to Couette flow. In comparing Eqs. (23) and (24), we find that velocity components of v^* and w^* increase in proportion to R_e and that the flow has a secondary flow.

Now, we introduce viscous frictional moment M, which is transmitted from the outer to the inner sphere. Considering the axial symmetry of flow, shear stress acting on the inner sphere $\tau_{r\phi}$ becomes

$$\tau_{r\phi}=\mu\{r\frac{\partial}{\partial r}(\frac{u}{r})\}_{r=R_1}=\frac{\mu R_1\omega}{s}[(1+\beta)\sin\theta + R_e^2\beta^4(1+\beta)^3 10^{-3}\{0.026455(1-\beta)\sin\theta + \frac{1}{2}(3\cos^2\theta-1)(0.70106\beta-1.2963)\sin\theta\}]. \tag{25}$$

Therefore

$$M=2\pi R_1^3\int_0^\pi \tau_{r\phi}\sin^2\theta d\theta=\frac{2\pi R_1^4\mu\omega}{s}\{\frac{4}{3}(1+\beta) + R_e^2\beta^4(1+\beta)^3 10^{-3}(0.38095-0.22222\beta)\}. \tag{26}$$

Hence, the coefficient of viscous frictional moment C_M becomes

$$C_M=\frac{8\pi}{3}\frac{(1+\beta)}{\beta}R_e^{-1}+2\pi(0.38095-0.22222\beta)\beta^3(1+\beta)^3 10^{-3}R_e. \tag{27}$$

The first term in Eq. (27) indicates the coefficient of viscous frictional moment obtained by the assumption of linear velocity distribution. The second term in Eq. (27) shows the increment of C_M induced by the secondary flow. Moreover, the dimensionless form of shear stress $\tau_{r\phi}^*$ is written by

$$\tau_{r\phi}^*=\frac{\tau_{r\phi}}{\rho R_1^2\omega^2}=\frac{(1+\beta)}{\beta R_e}[\sin\theta+R_e^2\beta^4(1+\beta)^2 10^{-3}\{0.026455(1-\beta)\sin\theta+\frac{1}{2}(3\cos^2\theta-1)(0.70106\beta-1.2963)\sin\theta\}]. \tag{28}$$

Now we shall consider the region of R_e and β, in which Eqs. (23) and (25)~(28) can be adopted. Substituting Eq. (22) into Eqs. (12) and (13) and setting up the condition of the convergency of Eqs. (12) and (13), the following relation can be obtained approximately by the order-of-magnitude calculation.

$$R_s\beta=R_e\beta^2<10. \tag{29}$$

3.2 WITH THE INNER SPHERE ROTATING

The boundary conditions are given by

$$\left.\begin{aligned} &u^*=\sin\theta,\ v^*=w^*=0 && \text{at } \eta=0,\\ &u^*=v^*=w^*=0 && \text{at } \eta=1.\end{aligned}\right\} \tag{30}$$

Rewriting the boundary conditions corresponding to both g_{jl} and f_{jl}, we can obtain at $\eta=0$:

$g_{jl}=0,\ dg_{jl}/d\eta=0,$ where both j and l are odd;

$f_{00}=1,\ f_{jl}=0,$ where both j and l are even except for 0; (31 a)

and at $\eta=1$,

$g_{jl}=0,\ dg_{jl}/d\eta=0,$ where both j and l are odd;

$f_{jl}=0,$ where both j and l are even. (31 b)

The functions g_{jl} and f_{jl} can be obtained in much the same way as in the foregoing paragraph.

$$f_{00}=1-\eta, \tag{32 a}$$

$$g_{02}=\beta^2\{-\frac{\beta}{180}\eta^6+\frac{1}{30}(\frac{1}{2}+\beta)\eta^5-\frac{1}{12}(1+\beta)\eta^4+\frac{4}{45}(\frac{21}{16}+\beta)\eta^3-\frac{1}{30}(\frac{3}{2}+\beta)\eta^2\}, \tag{32 b}$$

$$f_{02}=\beta^2 10^{-3}\{-0.39683\beta\eta^8+(1.32275+3.1746\beta)\eta^7-(9.25927+11.1111\beta)\eta^6+(22.7778+20.0\beta)\eta^5-(25.0+18.5185\beta)\eta^4+(11.1111+7.4074\beta)\eta^3-(0.95238+0.55556\beta)\eta\}, \tag{32 c}$$

$$f_{22}=\beta^2 10^{-3}\{-0.59524\beta\eta^8+(1.85185+4.7619\beta)\eta^7-(12.9629+16.6667\beta)\eta^6+(33.8889+31.1111\beta)\eta^5-(41.6667+31.4815\beta)\eta^4+(22.2222+14.8148\beta)\eta^3-(3.3333+2.5\beta)\eta\}, \tag{32 d}$$

$$g_{13}=\beta^4 10^{-5}\{-0.06124\beta\eta^{12}+(-0.108226+0.940624\beta)\eta^{11}+(1.19048-5.2263\beta)\eta^{10}+(-5.6217+12.6837\beta)\eta^9+(15.2778-11.9365\beta)\eta^8+(-23.4127+22.7337\beta)\eta^7+(13.8889-6.9842\beta)\eta^6+(14.2858+10.582\beta)\eta^5-(35.7143+3.70375\beta)\eta^4+(29.2146-108.095\beta)\eta^3+(-9.00065+81.659\beta)\eta^2\}, \tag{32 e}$$

$$g_{33}=\beta^4 10^{-5}\{-0.12804\beta\eta^{12}+(-0.112233+1.14373\beta)\eta^{11}+(1.23457-4.2975\beta)\eta^{10}+(-6.17284+6.3859\beta)\eta^9+(17.4603+13.9506\beta)\eta^8-(28.5714+7.3016\beta)\eta^7+(22.2222+7.7778\beta)\eta^6+(3.3333+8.3333\beta)\eta^5-(16.6667+12.5\beta)\eta^4+(6.8831-97.642\beta)\eta^3+(0.38959+84.278\beta)\eta^2\}. \tag{32 f}$$

The coefficient of viscous frictional moment C_M becomes

$$C_M=\frac{8\pi}{3}\frac{1+\beta}{\beta}R_e^{-1}+2\pi(0.38095+0.07413\beta)\beta^3 10^{-3}R_e. \tag{33}$$

The first term in Eq. (33) indicates the coefficient of viscous frictional moment obtained by the assumption of linear velocity distribution.

4. DISCUSSION

Fig. 2, in which clearance is magnified 25 times on the radius scale, provides an example of a contour line of the stream function Ψ^*, i. e.

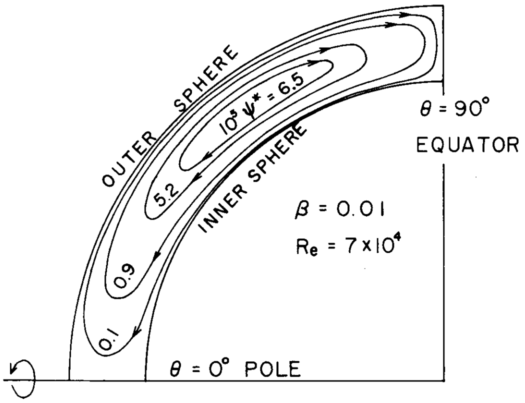

Fig. 2 Stream lines for $\beta=0.01$ and $R_e=7\times10^4$ (The clearance is magnified 25 times on the radius scale)

the stream line of secondary flow in the case where the outer sphere rotates and the inner one is stationary. In the case where the inner sphere rotates, the secondary flow direction is inverse in the case where the outer sphere rotates, but the effects of Reynolds number and clearance ratio on the velocity components and the shearing stress etc. seem to be the same as those in the case where the outer sphere rotates. Hence, in the following, the results of numerical calculation are discussed for the case where the outer sphere rotates.

Fig. 3 (a) shows the velocity distribution of the velocity component in the θ-direction v^*. It may be observed in Fig. 2 and 3 (a) that the secondary flow, $v^*>0$, from the pole ($\theta=0°$) to the equator ($\theta=90°$) occurs near the outer sphere wall region ($\eta>0.53$), while the secondary flow, $v^*<0$, from the equator to the pole occurs near the inner sphere wall region. The distributions of v^* at various θ show its increase with θ to $\theta=45°$. Having the maximum positive and negative values at $\theta=45°$, v^* decreases with an increase of θ, and becomes zero at $\theta=0°$. In the case of a small

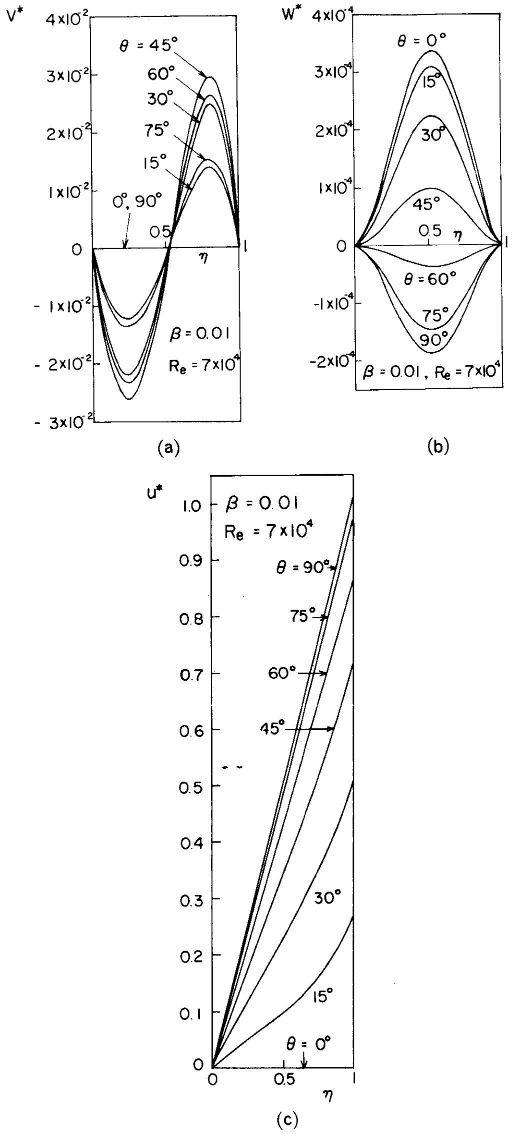

Fig. 3 (a)(b)(c) Dimensionless velocity distributions with θ as a parameter for a fixed value of R_e and β.

value of R_e β^2, it may be noted that the relationship between v^* and θ can be approximately given by $sin2\theta$.

The velocity component w^* in the r-direction, as shown in Fig. 3 (b) has a maximum value near $\eta=0.5$ for each θ. For $\theta<55°$, w^* is positive, i. e. a flow is observed from the wall of the inner sphere to that of the outer one; with $\theta<55°$, w^* is negative, i. e. flows opposite to that for $\theta<55°$, while w^* has positive and negative maximum values at $\theta=0°$ and 90°, respectively. In the case of a small value of $R_e\beta^2$, w^* is approximately proportional to $(3cos^2\theta-1)$.

The velocity component in the ϕ-direction u^* is shown for various θ in Fig. 3(c). For $\theta<55°$, the velocity distributions of u^* tend to make u^* at $\eta=0.5$ decrease from the linear distribution, because fluid near the wall of the inner sphere flows into the center of the space, accompanied by a smaller moment of momentum. On the other hand, the velocity distributions of u^* for $\theta>55°$ tend to make u^* at $\eta=0.5$ increase from the linear distribution, because fluid near the wall of

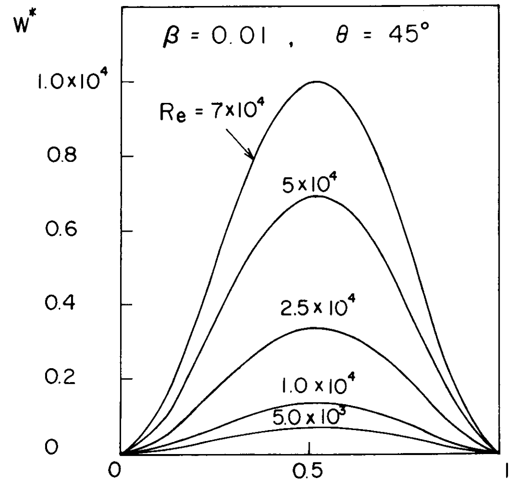

(b)

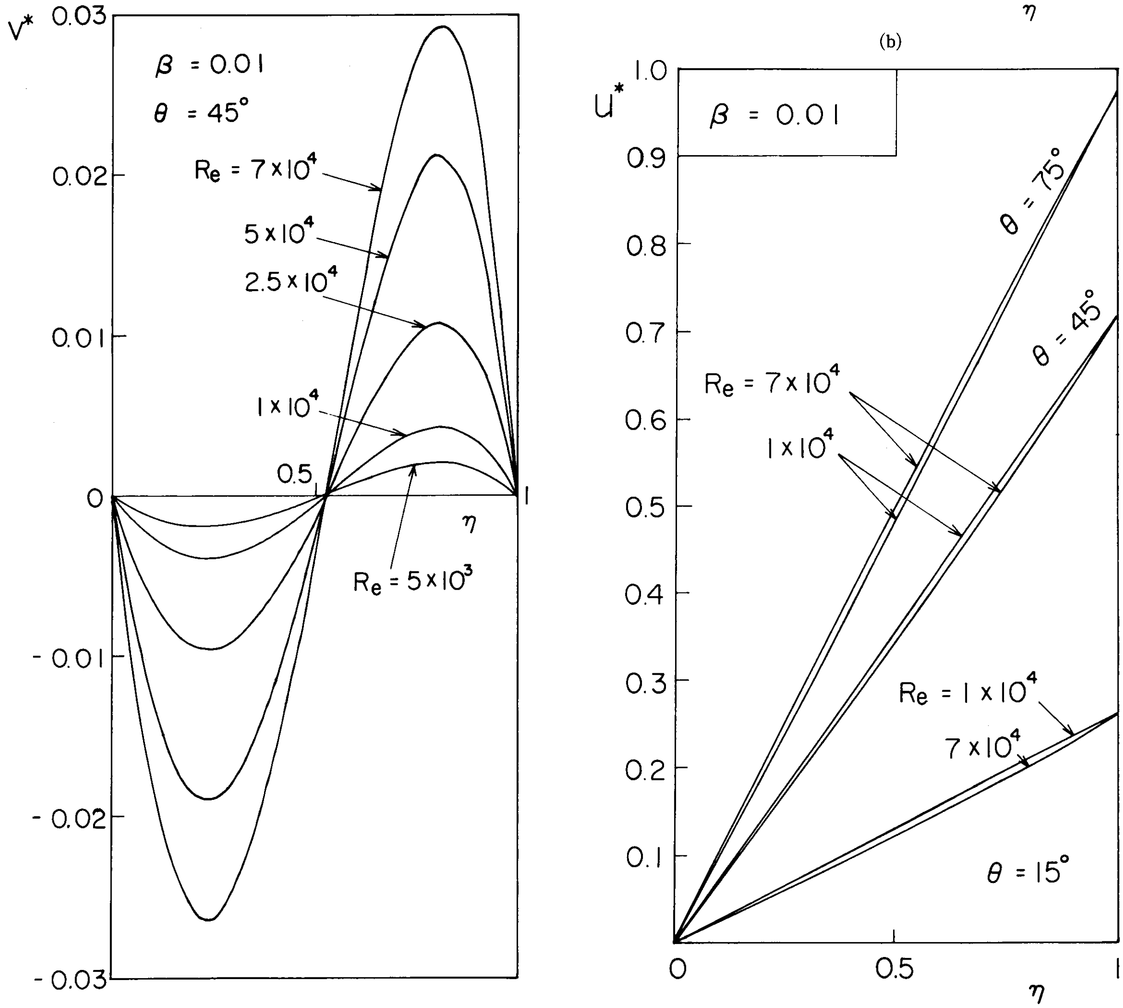

(a)　(c)

Fig. 4　(a)(b)(c) Dimensionless velocity distributions with R_e as a parameter for a fixed value of θ and β.

the outer sphere is accompanied by a greater moment of momentum in the center of the space. In other words, $w^* < 0$.

In creeping motion, where Reynolds number is extremely small, no secondary flow occurs. But in the flow-region of a large Reynolds numder, a secondary flow occurs whose velocity components v^* and w^* increase with R_e, as shown in Fig. 4 (a) and (b). But velocity component u^* is slightly influenced by R_e increase. The tendency of u^* to differ with an increase of R_e at $\theta = 15^\circ$ and 45° as compared to $\theta = 75^\circ$, as shown in Fig. 4 (c), depends on the sign of w^*. Figure 5 shows an example of the distribution of dimensionless shearing stress.

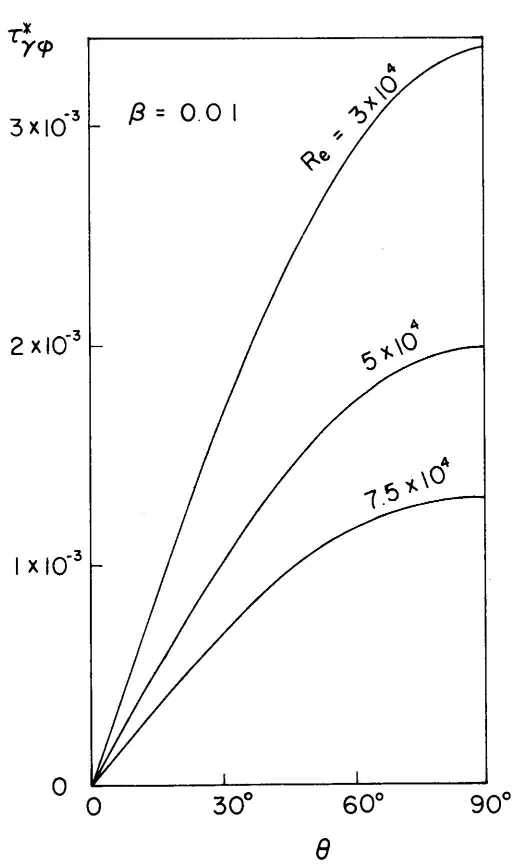

Fig. 5 Distribution of dimensionless shearing stress.

Now we try to compare the theoretical results with the experimental results for the coefficient of frictional moment C_M obtained by the auther (1978). In order to adapt the theoretical equation, Eq. (27), not only for a very small clearance ratio β, but for a relatively large β as well (but $\beta \ll 1$), the first term of Eq. (27) should be replaced by the solution of creeping motion, $C_M = 8\pi R_e^{-1}/\{1-(R_1/R_2)^3\}$. The following equation can be obtained.

$$C_M = \frac{8\pi}{1-(R_1/R_2)^3} R_e^{-1} + 2\pi(0.3805 - 0.2222\beta)\beta^3(1+\beta)^3 10^{-3} R_e. \quad (34)$$

In Fig. 6 Eq. (34) is compared with the experimental data which remain in the laminar flow region, Eq. (34) is in a good agreement with the experimental data, being within $R_e\beta^2 < 40$.

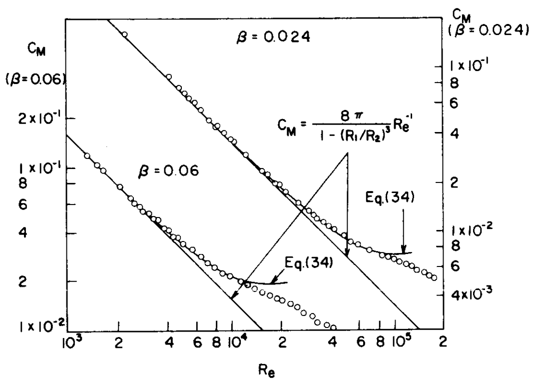

Fig. 6 Comparison between theory and experiment for C_M.

5. CONCLUSIONS

Only a velocity component in the ϕ-direction u^* exists in the creeping flow situation. But in the flow for large R_e, in addition to u, secondary velocity components v^* and w^* in the θ- and r-direction are also present. Both v^* and w^* increase approximately in proportion to R_e. But u^* is slightly influenced by R_e and the effect of R_e on u^* varies with θ, depending on the value of w^*. The relationship betweeen the order-of-magnitude of w^* and of v^* can be given by $w^*/v^* \sim \beta$, and that between v^* and u^* by $v^*/u^* \sim R_e\beta^2$. The coefficient of frictional moment is influenced a little, and it tends to increase for a large Reynolds number. The theoretical results agree well with the experimental data within $R_e\beta^2 < 40$.

REFERENCES

HOWARTH, L. 1951 Note on the boundary layer on a rotating sphere. *Phil. Mag.* **42**, 1308.

MUNSON, B. R. and JOSEPH, D. D. 1971 A viscous incompressible flow between concentric rotating spheres. part 1. Basic flow. *J. Fluid Mech.* **49**, 289.

NAKABAYASHI, K. 1978 Frictional moment of flow between two concentric spheres, one of which rotates. Trans. ASME, J. Fluid Eng. **100**, 97.

PEARSON, C. E. 1967 A numerical study of the time-dependent viscous flow between two rotating spheres. *J. Fluid Mech.* **28**, 323

SAWATZKI, O. and ZIEREP, J. 1970 Flow between a fixed outer sphere and a concentric rotating inner sphere. *Acta Mechanica,* **9**, 13.